

Fiber Bragg Grating Sensing for the Connection Failure of Fiber Reinforced Polymer Composite Structures

Seishi YAMADA*, Iwao KOMIYA**, Yukihiro MATSUMOTO*** and Takashi HIRAMOTO****

* Professor, PhD in Eng, *** PhD Student, **** Mc Student
Department of Architecture and Civil Engineering, Toyohashi University of Technology,
Hibarigaoka 1-1, Tempaku-cho, Toyohashi 441-8580, Japan

** Chief Researcher, Fukui Fibertech Co., Iwanishi 5-1, Nakahara-cho, Toyohashi 441-3196, Japan

This study deals with the rational joint system of FRP bridges and the structural health monitoring. In an alternative long-lived, maintenance-free FRP bridge, an innovative fiber optic sensing using fiber Bragg grating (FBG) sensors may now be hoped to avoid the risk by material damage. The longitudinal tensile tests of bolted or bonded lap FRP joints by the author and his co-workers, have shown that strain quantities of FRP members are able to be precisely measured and that the shapes of optical power spectra change into those with two peaks at the criteria related to the occurrences of micro cracks in the FRP members. This characteristic may be applied to the structural assessment for the occurrence of material micro-damages into the FRP material.

Key Words: Pultruded FRP, Tensile Test, FBG Sensor, Optical Power Spectrum

1. Introduction

Fiber reinforced polymer (FRP) composite material has high corrosion resistant, lightweight and high strength characteristics. And the long-lived FRP structure is very attractive to reduce the environmental burden that carbon dioxide emissions in the fabrication process are much smaller than other conventional structures. Many FRP bridges and FRP framed architectural structures have been reported by Burgoyne¹⁾ and Keller²⁾, however, it has not been enough to study the fundamental experiments for application to the practical design of bridges.

On the other hand, civil structures are the most important facilities for human activity. However, they usually have strong impacts to the environment of the earth. Thus, structural health and the damage identification should be assessed after various natural disasters. This kind of structural health monitoring requires an alternative long-time, high accuracy and stable sensor. The girders of Taylor Bridge in Canada³⁾ have been reinforced with FRP material and installed fiber optic sensors, and the live measuring data of these are now opened on the website by Intelligent Sensing for Innovative Structures in Canada.

In this study, recently developed fiber Bragg grating (FBG) sensors were embedded in FRP structural members⁴⁾. The structural health monitoring using optical FBG sensors has shown to give not only high accuracy strain data but also optical power spectra^{4,5)}. First, the longitudinal tensile test of the bolted or bonded lap joints of FRP strips have been carried out; torque free or 45N·m torque has been adopted in the present paper and the effects of frictional resistance capacity have been discussed. Second, the FBG sensors were embedded on the transverse direction of tensile test of the joints between FRP structural members. It is shown that the optical power decreases as the load increases, and its shape has two peaks after reaching at a critical load. When the optical power spectrum has two peaks, the strain responses have changed like two different FBG sensors due to the occurrences of small transverse cracks inside the FRP material under locally large stress concentration.

2. FRP Material

The adopted pultruded glass FRP plates are of the thickness $t=5.5\text{mm}$, and cut from the flanges of a $100\text{mm} \times 100\text{mm}$ box shaped section. The pultruded section consists of

two continuous fiber layers (28.3 vol%), three continuous strand mats (10.2 vol%) and two surfacing veils. In this study, the longitudinal x -direction is defined to be parallel to the continuous fiber. The longitudinal elastic modulus, E_x , the transverse elastic modulus, E_y , and the longitudinal tensile strength, σ_x , have been identified by using the same ways as shown in Ref.6; $E_x=22.1\text{GPa}$, $E_y=11.5\text{GPa}$ and $\sigma_x=347\text{MPa}$. The transverse elastic modulus are approximately half of those in the x -direction.

3. Experimental Method

3.1 Experimental Specimen

Figure 1 shows the schematic setup of the bolted or bonded lap joint configuration. The edge distance and the spacing were determined as Ref 7. In the cases of the bolted lap joint specimen, the FBG sensor was embedded beside the bolthole shown in Fig. 1 (a). In the case of the bonded one, the FBG sensor was embedded center of the jointed area shown in Fig. 1 (b). A groove was chiseled in the pultruded FRP member, and the FBG sensor was embedded into the groove using epoxy resin.

In this study, the torque free condition, T00, the 45Nm torque condition, T45, and bonded joints using epoxy resin, BD01 and BD02, were adopted to study the effect of the frictional resistance and also the joint efficiency.

3.2 Fiber Optic Sensing System

The fiber optic sensors in this study were of fiber Bragg grating (FBG) sensor. The FBG sensor consists of the clad and the core in which the simple intrinsic elements called Bragg diffraction grating are photo-imprinted shown in Fig. 2. The sensor length is 10mm and the grating pitch, Λ , is 500nm. The strain response arises due to the elongation of the sensor which corresponds to fractional change in grating pitch. Also the dependence of the Bragg wavelength on temperature arises due to both the dependence of the index of refraction of the glass and the thermal expansion of the glass. In this measurement, the applied strain, ε , is given by following equation.

$$\varepsilon[\mu] = 833[\mu/\text{nm}] \times (\Delta\lambda_B[\text{nm}] - K[\text{nm}/^\circ\text{C}]\Delta T[^\circ\text{C}])$$

where $\Delta\lambda_B$ is the shift in Bragg wavelength with strain, K revision coefficient for temperature and ΔT the value of temperature changing. In the present sensors, K is $0.010\text{nm}/^\circ\text{C}$.

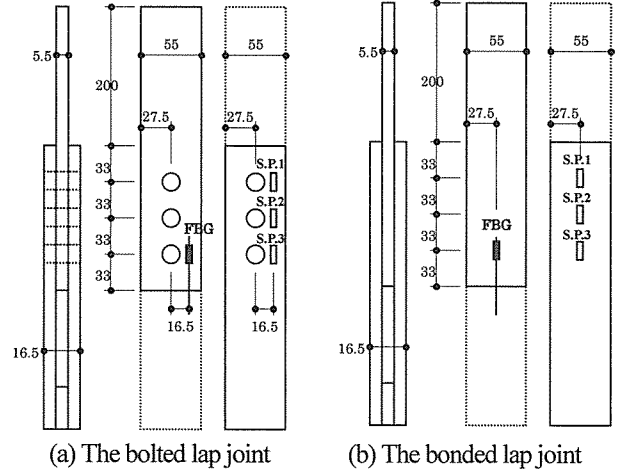


Fig.1 Setup of Specimens

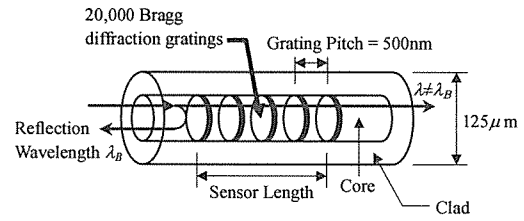


Fig.2 FBG Sensor

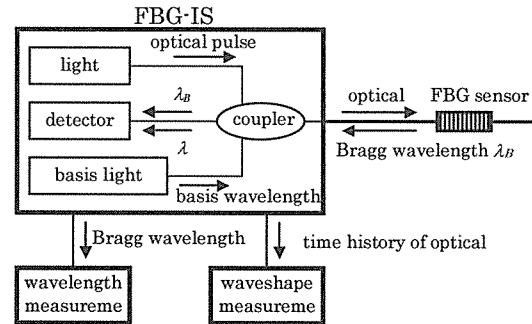


Fig.3 Diagram of Measurement System

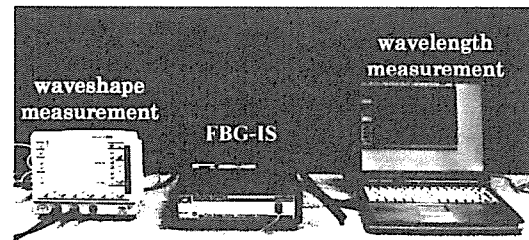
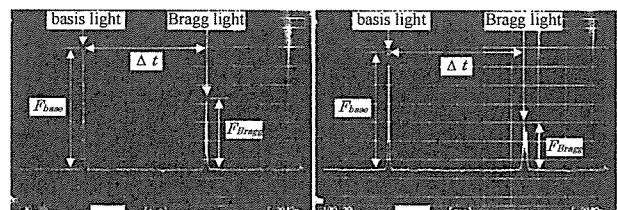


Fig.4 Measurement System



(a) $\varepsilon=0\mu$ (b) $\varepsilon=2000\mu$

Fig.5 Time History of Optical Power

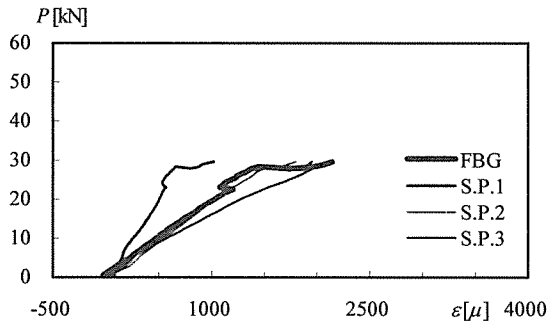
Figure 3 shows the schematic diagram of the strain measurement system; the main equipment, FBG-IS, consists of the input of light with a broadband spectrum and the wavelength detection system of the narrowband component reflected by the FBG. It is connected to the wavelength monitor and the waveshape monitor shown in Fig. 4.

Figure 5 shows an example of waveshape measurement. The basis light is invariable at all times, the time difference, Δt , between the peak time of the basis light and that of the Bragg light is directly related to the wavelength measurement.

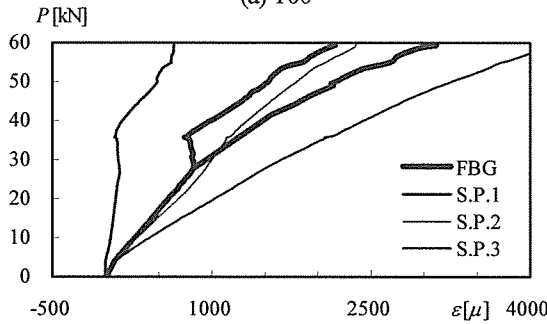
4. Experimental Results

4.1 Results of Bolted Lap Joints

Figure 6 shows the tensile load versus the strain plots. The ultimate load of T45 is approximately two times as large as



(a) T00



(b) T45

Fig.6 Load versus Strain Curves for Bolted Lap Joint

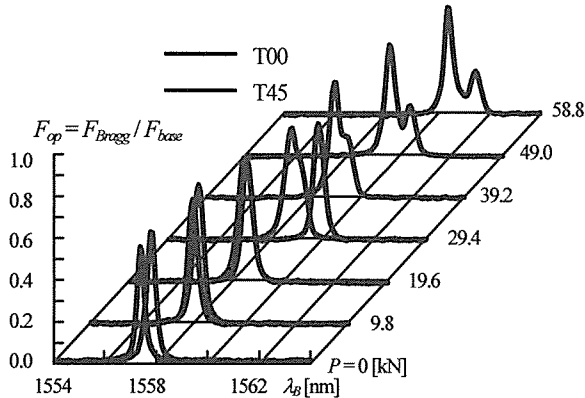
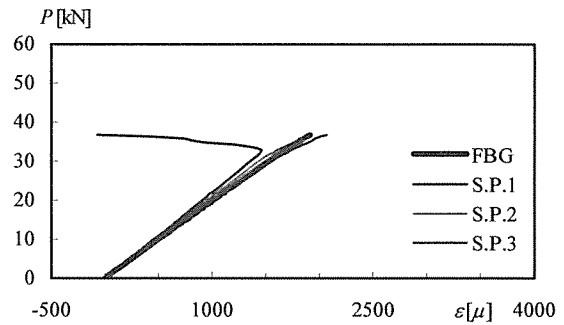


Fig.7 Optical Power Spectra in Bolted Lap Joint

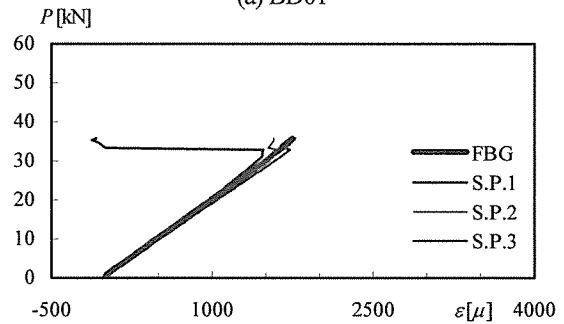
that of T00. The strain curve obtained from FBG sensor was almost the same as the conventional strain gauge, S.P.2, as shown in Fig.6. Figure 7 shows the variations of optical power spectra. In the case of T00, no change of the shape was observed. On the other hand, the shape in T45 had two peaks after reaching at critical load, and the strain value is 0.15%. These results mean that the development of micro damage inside FRP members can be procrastinated by increasing the frictional load transfer through bolt tightening.

4.2 Results of Bonded Lap Joints

Figure 8 shows the tensile load versus the strain plots. The ultimate load of the bonded lap joint specimens is larger than that of T00, but smaller than T45. The same as the case of the bolted lap joint, the strain curve obtained from FBG sensor was almost the same as the strain gauge, S.P.2, as shown in



(a) BD01



(b) BD02

Fig.8 Load versus Strain Curve for Bonded Lap Joint

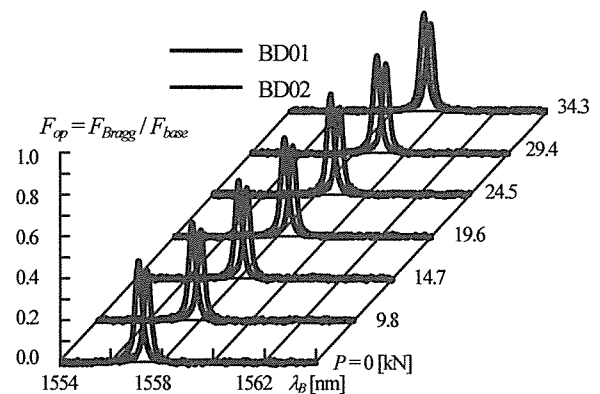


Fig.9 Optical Power Spectra in Bonded Lap Joint

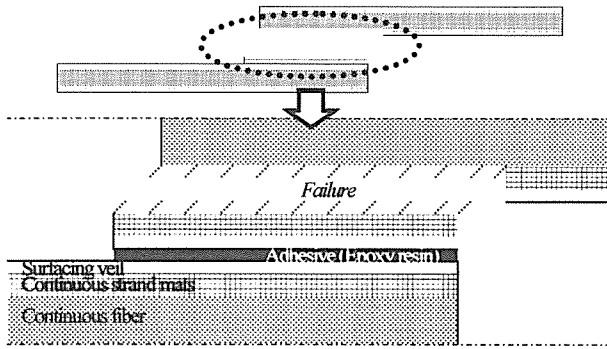


Fig.10 Failure Condition for Bonded Lap Joint

Fig.8. Also the stable $P-\varepsilon$ curves were obtained until the load reaches an ultimate load. Figure 9 shows the variations of optical power spectra. In the case of the bonded lap joint, no change of the shape was observed. The delamination failure occurred at the boundary between continuous strand mat layers and continuous fiber layer fiber shown in Fig.10.

4.3 Joint Efficiency

Shown in Fig. 11 are the joint efficiency C_{JE} , the ratio of the ultimate load obtained by tensile test to the tensile strength of the FRP member σ_x ; in the present study, the joint efficiency, C_{JE} , is defined by the followings,

$$C_{JE} = \frac{P_{\max}^{\text{test}}}{(t \times w \times \sigma_x)} = \frac{P_{\max}^{\text{test}}}{(5.5[\text{mm}] \times 55[\text{mm}] \times 247[\text{N/mm}^2])}$$

where P_{\max}^{test} is the ultimate load obtained by tensile tests. The ultimate load of T45 is approximately half as many as that of the FRP member. And also the ultimate load of T00, BD01 and BD02 are approximately half as many as that of T45. It is suggested in Fig.11 that the combined bolted and bonded joint is appropriate for the higher joint strength.

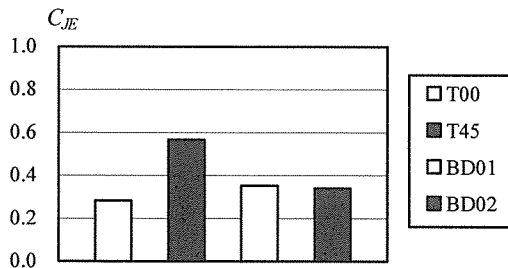


Fig.11 Joint Efficiency

5. Conclusions

In the present paper, an innovative fiber optic sensing for the various joints of the pultruded FRP structures have been investigated. The fiber optic sensors in this study were of fiber Bragg grating (FBG) sensor.

The strain output detail of the FBG sensors embedded into the pultruded FRP members has been measured. And the strain response has been recognized to be approximately the same as that of the conventional electric strain gauge.

The bifurcation behavior of the Bragg wavelength, which related to the change of the waveshape, has been obtained. Then the optical power, which obtained waveshape measurements, decreased rapidly, and its shape changed from sharp one-peak to two-peak one because of the occurrence of small transverse cracks inside the pultruded FRP member. In the case of the longitudinal tensile test of bolted lap joints, the bifurcation strain is one-third of the ultimate strain of FRP members. However, in the case of bonded lap a joint, the bifurcation behavior was not obtained because the strain did not reach to the critical strain for the small transverse cracks because the delamination occurred at the boundary between continuous strand mat layers and continuous fiber layer.

It has been shown that the optical power waveshape has changed due to the accumulation of the micro cracks in the FRP member. It is believed that the present FBG sensing would contribute to not only the FRP members but also wide classes of buildings or civil engineering structures.

Acknowledgement

This study is the part of the 21st Century COE Program (Toyohashi University of Technology): Ecological Engineering for Homeostatic Human Activities adopted by the Ministry of Education, Culture, Science, Sports and Technology, Japan, in 2002.

References

- 1) Burgoyne, C.J.: Advanced composites in civil engineering in Europe, SEI, IABSE, 267-273, 1999
- 2) Keller, T.: Overview of fiber-reinforced polymers in bridge construction, SEI, IABSE, 66-70, 2002
- 3) <http://www.isiscanada.com>
- 4) Yamada, S., Nakazawa, H.Y., Komiya, I. and Matsumoto, Y.: Fiber Bragg grating sensing for long-lived fiber reinforced polymer structures, Proc. IABSE, 3S, SHA220, 1-6, 2004
- 5) Yamada, S., Matsumoto, Y., Hiramoto, T. and Yamada, S.: Fiber optic sensing for steel bridges, AESE2005, 2, 627-632, 2005.
- 6) Yamada, S. and Komiya, I.: Elastic deflection behavior of a box-shaped pultruded composite member and its collapse, Fiber Composites in Infrastructure, ICCI'96, 699-707, 1996
- 7) Yamada, S., Nakazawa, H.Y., Fukatsu, N. and Komiya, I.: Experiment on the connection collapse of pultruded fiber reinforced polymeric composites, CD-ROM Proc. IASS, TP071, 2001